J. Appl. Cryst. (1993). **26**, 295–302

PEDX: a program for radial-distribution-function analysis of energy-dispersive X-ray diffraction data from disordered systems.

By V. Petkov,* *Kimura Metamelt Project, ERATO, JRDC, c/o Research Institute for Electric and Magnetic Materials*, 2-1-1 *Yagiyama-minami, Taihaku-ku, Sendai* 982, *Japan*, and Y. Waseda, *Institute for Advanced Materials Processing, Tohoku University, Sendai* 980, *Japan*

(*Received* 9 *July* 1992; *accepted* 6 *October* 1992)

Abstract

PEDX is a newly developed interactive computer program for the radial-distribution-function analysis of measured energy-dispersive X-ray diffraction (EDXD) data from disordered systems. The program is furnished with efficient computing procedures and all the standard data for 96 neutral atoms necessary for the calculations. With the help of *PEDX*, the rather involved EDXD data processing is reduced to a routine operation.

1. Introduction

The atomic-scale structure of a disordered system such as a liquid or a glass is commonly described in terms of the radial distribution function (RDF). The widely used reduced RDF, $G(r)$, which gives the probability of finding an atom at a distance r from a reference atom, is defined as

$$G(r) = 4\pi r[\rho(r) - \rho_0], \tag{1}$$

where r is the radial distance and $\rho(r)$ and ρ_0 are the local and the average atomic number densities, respectively. The reduced RDF corresponds to the Fourier transform of only the coherent diffraction spectrum of a disordered system, *i.e.*

$$G(r) = (2/\pi)\int_0^\infty s[i(s) - 1] \sin(sr)\, ds, \tag{2}$$

where $i(s)$ is the so-called interference function, obtained directly from a diffraction experiment by properly correcting and normalizing the coherent X-ray scattering intensities, and s is the wave vector defined by the relation $s = (4\pi/\lambda)\sin\theta = (4\pi/hc)E\sin\theta$. λ and E are the wavelength and the energy of the radiation used, h is Planck's constant, c is the velocity of light and 2θ is the angle between the directions of the incident and diffracted X-rays. In order to calculate the RDF, the coherent X-ray scattering intensity as a function of s, $I = I(s)$, has to be experimentally obtained from a system of interest and properly reduced to $i = i(s)$, which is an immediate task for any structural study of disordered systems. There are two experimental approaches to this task, since the wave vector s is a function of both diffraction angle and energy. With so-called 'angle-dispersive X-ray diffraction' (ADXD), usually employed in the past, the dependence of the scattered intensity on s is obtained by using monochromatic radiation (λ = constant, E = constant) and varying the diffraction angle 2θ. In principle, the same functional dependence can be detected by utilizing white radiation with a continuous energy spectrum (λ, $E \neq$ constant) and keeping the diffraction angle fixed. This experimental approach has been called 'energy-dispersive X-ray diffraction' (EDXD), since the diffracted intensities are recorded as a function of energy, E. Several important advantages of EDXD over conventional ADXD can be outlined. Relatively rapid data collection is possible because: the total intensity of the white radiation is higher than that of the characteristic monochromatic radiation; fluctuations in the X-ray source do not affect the experimental data quality since all diffracted X-ray photons of different energies are collected simultaneously; no mechanical moving parts are required since the energy scanning is done electronically by the detector system. This results in freedom from the danger of optical misalignment. The use of higher energies, up to 50 keV, makes it possible to obtain the diffraction spectrum and consequently the interference function in the higher-wave-vector region up to 25 $Å^{-1}$. It may be noted, for comparison, that the energy of the most commonly used Mo $K\alpha$ characteristic radiation is 17.48 keV, so with the ADXD method the interference function is usually obtained up to 16 $Å^{-1}$ only. The latter advantage of EDXD is quite significant, since the larger the range of s over which $i(s)$ values are obtained, the better the resolution of the corresponding radial distribution function and, hence, the more detailed the structural features of the disordered system under study that can be revealed.

Several researchers have demonstrated the advantages of EDXD in studying disordered systems. In their pioneering work, Prober & Schultz (1975) determined the structure of liquid mercury. Murata & Nishikawa (1978) and Nishikawa & Iijima (1984) have studied the structure of liquid CCl_4 with the greatest possible care. The structure changes of liquid bismuth during its solidification have been investigated by Momiuchi (1986). Tamura (1990) and Hosokawa, Matsuoka & Tamura (1991) have employed the EDXD method in a high-pressure study of the structure of liquid selenium and mercury. Radial distribution analysis of a series of oxide glasses has been carried out by Ozawa & Uno (1986), Hanson & Egami (1986) and McKeown (1987). Structural studies of various metallic glasses have been reported by Egami (1978, 1979) and Aur & Egami (1980). Other investigations have been carried out by Wagner, Lee, Tai & Keller (1981), Hoving, Egami, Vincze & Woude (1987) and Utz, Brunsch, Lamparter & Steeb (1989).

Two experimental problems, however, prevent us from completely fulfilling the attractive potential of EDXD. The first is a result of the relative complexity

* Permanent address for correspondence: Department of Solid State Physics, Sofia University, Sofia 1126, Bulgaria.

0021-8898/93/020295-08$06.00

of the EDXD equipment system. With EDXD, the diffracted radiation is detected by an energy-sensitive detector, which must possess a good energy resolution. This has been a problem. However, with the advance of modern semiconductor technology, solid-state detectors (Li-drifted Si and intrinsic Ge) with energy resolutions $\Delta E/E$ of a few percent, which are quite satisfactory for structural studies on disordered systems, have become commercially available. The same situation holds for the complex electronics units (amplifier, multichannel pulse-height analyzer *etc.*) complementary to the detector. Thus, the problem of the experimental set-up has been overcome and the EDXD equipment can be assembled without much difficulty at present. The second problem arises from the fact that the measured EDXD spectrum consists of diffracted X-ray photons of different energies, which makes the data processing quite involved. Some pioneering procedures for EDXD data processing have already been developed in computer programs (Aur, 1981; Hoving, 1986). However, these have been oriented towards some specific research demands and are not always convenient for general use. It is the purpose of the present work to develop proper computational procedures for EDXD data processing, which, coupled with the available EDXD equipment, will make EDXD studies on disordered systems as easy and routine as conventional ADXD.

2. Theoretical background

The total intensity of X-rays scattered from a sample and its environment, as a function of energy E (*i.e.* of wave vector s), at a fixed diffraction angle 2θ, is given by

$$I(E, \theta) = C(E)\varepsilon(E)[I_{coh}(E, \theta) + I_{inc}(E, E', \theta) + I_{ms}(E, E', \theta) + I_{air}(E, \theta) + I_{cell}(E, \theta)], \quad (3)$$

where $C(E)$ is a normalization factor; $\varepsilon(E)$ is the detector efficiency factor; the first three terms in the brackets refer to the intensities of coherent (single), incoherent (single) and multiple scattering from the sample, respectively; the last two terms refer to those scattered by air and the sample container, respectively; E' is the initial energy of the incoming X-ray photons, which is reduced to E in the incoherent (Compton) scattering process. The relation between E and E' can conveniently be expressed by

$$E' = E/[1 - 0.00392(E \sin^2 \theta)] \quad (4)$$

if E and E' are given in units of keV (Wagner, 1978).

The quantity of interest is the intensity scattered by the sample alone, so the total EDXD spectrum has to be corrected for the scattering due to the specific sample environment. In this program, the air and container scattering corrections are performed by well established and commonly applied procedures (Wagner, 1978; Waseda, 1980, pp. 27–36). They are not reproduced here since they have been described in detail in the literature referred to.

Another contribution to the total EDXD experimental spectrum that must be accounted for is the result of double, triple and higher-order scattering, *i.e.* radiation that, before reaching the detector, has been scattered two or more times by different volume elements in the sample. We considered only the doubly scattered radiation, since it represents the major part of the multiple scattering. The approximate numerical integration method developed by Malet, Cabos, Escande & Delord (1973) was employed for calculating the ratio of the intensities of double and single coherent scattering. The quite complex mathematical expressions are not duplicated here. An estimate for the significance of the multiple-scattering correction in EDXD data analysis is given in the next section.

The EDXD spectrum contains contributions from both coherently and incoherently singly scattered X-ray photons, *i.e.* some fraction of all the detected photons of energy E comes from incoherently scattered photons with initial energy E', which is larger than E. The incoherent singly scattered intensity $I_{inc}(E, E', \theta)$ can be calculated using

$$I_{inc}(E, E', \theta) = I_0(E')A(E, E', \theta)P(E, E', \theta) \times R(E, E')(dE'/dE)I^a_{inc}(s'), \quad (5)$$

where $I_0(E')$ is the incident X-ray beam intensity; $A(E, E', \theta)$ and $P(E, E', \theta)$ are absorption and polarization correction factors, respectively; $R(E, E')$ is the Breit–Dirac recoil factor; dE'/dE is a correction factor accounting for the incoherent EDXD spectrum contraction; $I^a_{inc}(s')$ is the incoherent singly scattered intensity per atom; s' is the length of the wave vector, $s' = (4\pi/hc)E' \sin \theta$. It has been shown that the correction factor dE'/dE exactly cancels the Breit–Dirac recoil factor $R(E, E')$, so $d(E'/dE)R(E, E') = 1$ for the EDXD experiment (Egami, 1978).

The polarization factor for a continuous energy X-rays can be written as follows (Aur, 1981):

$$P(E, E', \theta) = [(E/E') + (E'/E) - \sin^2 2\theta]/2 + [\pi(E) \sin^2 2\theta]/2, \quad (6)$$

where $\pi(E)$ is a measure of the degree of polarization of the incident white X-rays. When a sealed tube is used as an X-ray source, it is customary for it to be tilted at 45° to the plane of the incident and diffracted X-ray beams in order to get rid of the energy dependence of the polarization factor (Olsen, Buras, Jensen, Alstrup, Gerward & Selsmark, 1978; Egami, 1979). In addition to this standard experimental case when $\pi(E) = 0$, we have also included the cases when $\pi(E) = \pm 1$, which correspond to synchrotron-radiation diffraction experiments carried out in vertical and horizontal scattering planes, respectively, as options in the present version of the program.

Analytical expressions of the absorption factor $A(E, E', \theta)$, for both transmission and reflection geometry, are taken from Wagner's (1978) scheme. A knowledge of the energy dependence of the linear absorption coefficients, $\mu = \mu(E)$, is, however, a prerequisite to their application. Mass absorption coefficients μ/ρ and X-ray anomalous-dispersion factors f' and f'' for 96 neutral atoms have been estimated in the energy range between 1 and 50 keV (Waseda, 1984) and are available as numerical data. On the basis of these values we created a compact data base (500 kbytes; binary data format) containing $\mu(E)/\rho$ and $f'(E)$ and $f''(E)$ data for all atomic species

from lithium to californium. The coefficients of the analytical expressions for the usual atomic scattering factors, f^0, derived by Cromer & Waber (1965) have also been stored in the program *PEDX*. Accounting for the specific energy range and the sample composition, *PEDX* extracts from the data base and the table of f^0 values the data necessary for the calculations.

Theoretical values of $I^a_{inc}(s')$ have been calculated by Cromer & Mann (1967) and Cromer (1969) for all elements in the Periodic Table. On the basis of these values, Thijsse (1984) has derived a simple semiempirical computational expression for $I^a_{inc}(s')$ that has been used in the present program.

The coherent contribution to all the X-ray photons scattered once by the sample is

$$I_{coh}(E, \theta) = I_0(E)P(E, E, \theta)A(E, E, \theta)I^a_{coh}(s), \qquad (7)$$

where $I_0(E)$ is the intensity of the incident X-rays of energy E; $P(E, E, \theta)$ and $A(E, E, \theta)$ are the aforementioned polarization and absorption correction factors, respectively; and $I^a_{coh}(s)$ is the coherent singly scattered intensity per atom – the only structure-dependent part of the total EDXD spectrum. In order for $I^a_{coh}(s)$ to be determined, the coherent diffraction intensities, $I_{coh}(E, \theta)$, have to be extracted from the total experimental EDXD spectrum by accounting for all other contributions to it in the manner already described. Furthermore, the incident X-ray beam intensity $I_0(E)$, the detector efficiency $\varepsilon(E)$ and the normalization factor $C(E)$ must be known, since the coherent diffraction intensities are to be normalized against their product. Unfortunately, direct determination of $I_0(E)$ as a function of the photon energy E is not a easy task. It is particularly difficult to obtain $I_0(E)$ values with an accuracy sufficient for the structural determination of disordered systems (Nishikawa & Iijima, 1984; Uno & Ishigaki, 1984). However, some methods of estimating $I_0(E)$ quite accurately from the measured EDXD spectrum of the sample have been reported (Egami, 1978; Wagner, Lee, Tai & Keller, 1981; Fritch & Wagner, 1986) and the procedure proposed by Wagner, Lee, Tai & Keller (1981) was adopted in this program. The derivation of the quantity $I_p(E) = C(E)\varepsilon(E)I_0(E)$, hereafter referred to as the spectrum of the incident radiation beam, is described in more detail in §3.

3. Outline of the program *PEDX*

The program *PEDX* consists of five subroutines (*DATASET*, *BEAMCAL*, *DATACOR*, *INTERF* and *DISTRF*; see Fig. 1), in which separate steps of the radial-distribution-function analysis of measured EDXD data are performed.

3.1. *The DATASET subroutine*

The *DATASET* subroutine creates data files containing the values of standard physical quantities and the relevant experimental parameters involved in the computational scheme described in the previous section. Data, supplied by the user that describe the disordered system under study and the specific experimental conditions are included in a parameter data file. These data are as follows: the number of atomic species (up to six) constituting the sample; their atomic concentrations c_i and periodic atomic numbers; the average atomic density and the thickness of the sample; the same characteristic data for the sample substrate or container (if used); the type of geometry of the experimental set-up (both symmetrical reflection and transmission geometry are supported); the degree of polarization of the incident X-ray beam [$\pi(e) = 0, \mp 1$]; the use of additional filters. The parameter file also includes the number of channels (maximum 1024) of the multichannel pulse-height analyzer coupled to the solid-state detector and the energy-calibration constants necessary to convert a channel number into an appropriate energy value. The energy-calibration constants are either known *a priori* and supplied by the user or are calculated by *PEDX* on the basis of data extracted from standard EDXD spectra made up of X-ray fluorescent lines with accurately known energies. The energy-calibration constants stored in the parameter data file are obtained by the application of a linear least-squares fit of these known energies to the corresponding channel numbers.

In accordance with the characteristic data supplied to the parameter data file, the *DATASET* subroutine generates two supplementary data files, the first containing the mass absorption coefficients $\mu(E)/\rho$, the second the anomalous-dispersion factors $f'(E)$ and $f''(E)$ for the atomic species constituting the sample. The data are extracted from the data base described in §2.

With the solid-state detectors used in EDXD experiments, an escape-peak effect is observed which is due to the fluorescence of the detector material (Fukamachi, Togawa & Hosoya, 1973). The effect can be estimated by measuring the Bragg diffraction peaks and their escape peaks from a (mono)crystalline material. Once supplied with appropriate experimental data, the *DATASET* subroutine calculates and stores in a data file an escape-peak correction function. The correction of the EDXD data for the escape-peak effect is made in the subsequent steps of the data analysis with the use of the correction function in a way described by Aur (1981) and Nishikawa & Iijima (1984).

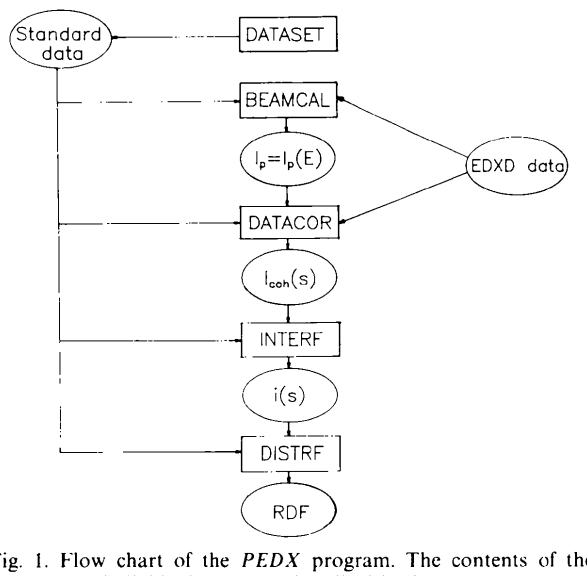

Fig. 1. Flow chart of the *PEDX* program. The contents of the individual steps are described in the text.

Additional filters placed in the incident or diffracted X-ray beams are sometimes used to cut out or reduce the strong fluorescent lines that interfere with the EDXD spectrum. The effect of filter absorption on the EDXD experimental data can be accounted for by measuring diffraction peaks from a well crystallized material with and without filters, calculating the ratio of the corresponding intensities as a function of energy (channel number) and subsequently multiplying the EDXD data by the correction function obtained. An option for calculating a filter-absorption correction function is provided in the *DATASET* subroutine. The necessary experimental data (pairs of Bragg diffraction intensities) are supplied by the user and the resulting correction function is stored in a separate data file.

All data files created in this step are given appropriate names by which they are automatically accessed in the course of the program execution. For convenience, all data input to the *PEDX* program are listed in Table 1.

Table 1. *Input data for the PEDX program*

Sample data
- Atomic numbers of the sample constituents
- Atomic concentrations of individual constituents
- Sample density and thickness

Experimental conditions
- Type of geometry.
- Degree of polarization of the incident radiation beam
- Number of channels
- Energy-calibration constants

Auxiliary data*
- Filter absorption
- Escape-peak effect

Experimental EDXD data
- EDXD data from the sample
- EDXD data from the sample environment*

*Optional.

3.2. *The BEAMCAL subroutine*

The spectrum of the incident radiation beam, $I_p = I_p(E)$, is calculated in the *BEAMCAL* subroutine. The method employed is that developed by Wagner, Lee, Tai & Keller (1981). It is based on the fact that the X-ray photons scattered by the sample are only a small fraction of the EDXD intensities obtained at higher diffraction angles (say $2\theta > 80°$), so the measured EDXD spectrum will show only small modulations about $I_p(E)$.

At higher diffraction angles, the coherent single scattering contribution to the EDXD spectrum, $I^a_{\rm coh}(s)$, can be well approximated by the so-called independent scattering.

$$\langle f^2\rangle = \sum c_i f_i^2(s, E) = \sum c_i[f^0(s) + f'(E)]_i^2 + \sum c_i[f''(E)]_i^2, \quad (8)$$

where $\{f^0(s); f'(E)\}_i$ and $f''(E)_i$ are the real and imaginary parts, respectively, of the atomic scattering factor $\{f(s, E)\}_i$ of the ith atomic species in the system of interest. With this assumption, (3) reduces to the following expression for large values of 2θ, *i.e.* of s:

$$I_{\rm cor}(E, \theta) = I_p(E)[A(E, E, \theta)P(E, E, \theta)\langle f^2\rangle + I_{\rm ms}(E, E, \theta)] + I_p(E')[A(E, E', \theta)P(E, E', \theta)I^a_{\rm inc}(s')], \quad (9)$$

where $I_{\rm cor}(E, \theta)$ is the EDXD intensity already corrected for air and sample-container scattering and $I_{\rm ms}(E, E, \theta)$ is the coherent multiple scattering term. This equation can be solved for the unknown quantity $I_p(E)$ and written in the following two equivalent forms:

$$I_p(E) = I_{\rm cor}(E, \theta)/\{A(E, E, \theta)P(E, E, \theta)\langle f^2\rangle + I_{\rm ms}(E, E, \theta) + I_p(E')/I_p(E)[A(E', E, \theta)P(E, E', \theta)I^a_{\rm inc}(s')]\}; \quad (10a)$$

$$I_p(E') = I_{\rm cor}(E, \theta)/\{A(E, E', \theta)P(E, E', \theta)I^a_{\rm inc}(s') + I_p(E)/I_p(E')[A(E, E, \theta)P(E, E, \theta)\langle f^2\rangle + I_{\rm ms}(E, E, \theta)]\}. \quad (10b)$$

When the coherent contribution to $I_{\rm cor}(E, \theta)$ dominates, which is the case for a system composed of heavy elements, the spectrum of the incident radiation beam is calculated on the basis of (10*a*), with the initial assumption that $I_p(E')/I_p(E) = 1$. On the other hand, when the system under study is composed of light atomic species, the incoherent contribution to $I_{\rm cor}(E, \theta)$ dominates and the spectrum of the incident radiation beam is calculated on the basis of (10*b*), with the initial assumption that $I_p(E)/I_p(E') = 0$. In both cases, the values of the spectrum of the incident radiation beam are refined through an iterative procedure (Wagner, Lee, Tai & Keller, 1981). The $I_p(E)$ data obtained are smoothed, approximated by a fifth-order polynomial function to eliminate spurious oscillations occurring at very low and very high energies and stored in a data file. The quality of the spectrum of the incident radiation beam calculated can be judged by the next step of the EDXD data analysis in which the same higher-angle EDXD data are corrected and normalized and a segment of the interference function $i(s)$ is calculated on their basis. Correct physical behavior of $i(s)$, which should oscillate uniformly around $i(s) = 1$, indicates that the $I_p(E)$ data are of good quality.

It should be emphasized that the spectrum of the incident radiation beam determined by the present method is highly dependent on the specific EDXD data used. Fig. 2 shows the spectrum of an X-ray beam emitted by a W tube (operated at 50 keV, 38 mA) obtained from the measured EDXD intensity of SiO_2 glass collected at $2\theta = 80°$ with and without the coherent multiple scattering term, $I_{\rm ms}(E, E, \theta)$, in the computational scheme. As one can see in Fig. 3, the coherent multiple (double) scattering contribution is a considerable fraction of the EDXD spectrum for the experimental conditions – symmetrical reflection geometry, 7 mm thick SiO_2 sample. However, the resultant $I_p(E)$ curves depicted in Fig. 2 are of a similar shape, although it should be noted that there is a difference of a few percent in their numerical values. The $I_p(E)$ values obtained from the EDXD intensity of liquid mercury are also shown in Fig. 2 and they are larger by almost one order of magnitude than those from silica glass. In summary, the spectrum of the incident radiation beam obtained from a measured EDXD intensity of a given sample can be used straightforwardly in the further EDXD data analysis

of the same sample only. In addition, the same EDXD data-correction procedure should be employed in both the derivation of the $I_p(E)$ values and the subsequent EDXD data processing.

3.3. *The DATACOR subroutine*

The correction of the raw EDXD data and the extraction from them of the structure-dependent part alone are performed by the *DATACOR* subroutine. With the EDXD experiments, the diffracted X-ray photons are detected by a solid-state detector and processed by a multichannel analyzer. The intensities obtained are in fact collected as a function of channel number, so these are transferred in energy space using the initially determined energy-calibration constants at first. Then the EDXD data are corrected for air and container scattering if proper supplementary experiments have been carried out. With the use of previously calculated correction functions, the filter absorption and escape-peak effect are properly accounted for. The incoherent and multiple-scattering contributions are (optionally) estimated (see §2) and subtracted from the corrected experimental data. The residual is just the coherently scattered intensities, which, after correction for polarization, absorption and rescaling against the incident radiation beam intensity $I_p(E)$, are converted to $I^a_{coh}(s)$. The coherent single scattering data, $I^a_{coh}(s)$, are smoothed by the well known method of Savitzky & Golay (1964), recalculated in equidistant steps of $\Delta s = 0.025$ Å^{-1} from $s_{min} = (1.0135E_{min}) \sin\theta$ to $s_{max} = (1.0135E_{max}) \sin\theta$, where E_{min} and E_{max} (in keV) are the minimum and maximum values, respectively, of the energy for which the spectrum of the incident radiation beam has been accurately determined. Finally, the most frequently used Faber–Ziman,

$$i_{FZ}(s) = \{I^a_{coh}(s) - [\sum c_i f_i^2 - (\sum c_i f_i)^2]\}/(\sum c_i f_i)^2, \quad (11)$$

or Ashcroft–Langreth,

$$i_{AL}(s) = I^a_{coh}(s)/\sum c_i f_i^2, \quad (12)$$

types of interference function (Waseda, 1980, pp. 7–17) are computed in the range of s values from s_{min} to s_{max} and stored in separate data files. Raw EDXD data and the corresponding segments of the Faber–Ziman-type interference function obtained by carrying out this step of the present EDXD data analysis are shown in Figs. 4 and 5 for SiO_2 glass.

3.4. *The INTERF subroutine*

Usually several (five to ten) scattering experiments at different but fixed diffraction angles 2θ are carried out for disordered systems by the EDXD method in order to cover as wide a range of s values as possible. The different segments of the interference function, each obtained from an EDXD data set collected at a different diffraction angle, are joined to each other, thus giving the total interference function, in the *INTERF* subroutine. The construction process starts with the $i(s)$ segment derived from the EDXD data used for the $I_p(E)$ determination as well. The next $i(s)$ segment, derived from the EDXD data obtained at the next lowest diffraction angle, is scaled to the first one and a new master $i(s)$ segment, an average value of the first and scaled second segments, is obtained. The scaling constant is determined through a least-squares regression analysis of the values of both segments in the overlapping region of s values. The procedure is repeated, considering the next $i(s)$ segments, until the total $i(s)$ function, of either the Faber–Ziman or the Ashcroft–Langreth type, is extended to the lowest s value covered by the EDXD experiments. The experimentally inaccessible part of $i(s)$, below this value, is derived by linear extrapolation to $s = 0$. The quality of the $i(s)$ function thus obtained

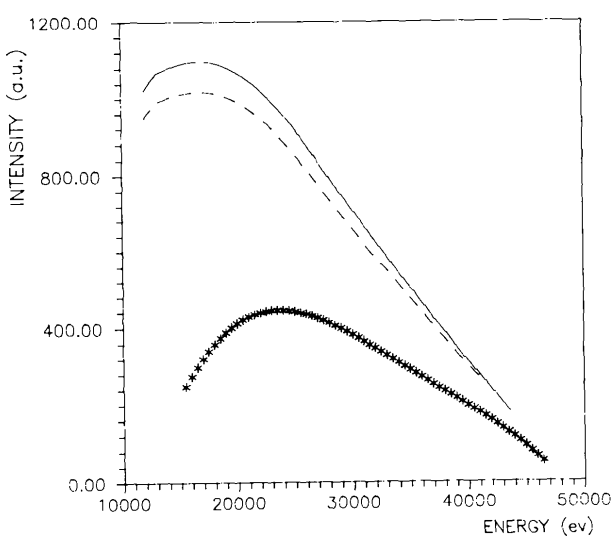

Fig. 2. Spectrum of the incident radiation beam of a W tube obtained from liquid mercury (* multiplied by 0.1); from SiO_2 glass corrected (– –) and not corrected (– – –) for coherent multiple scattering.

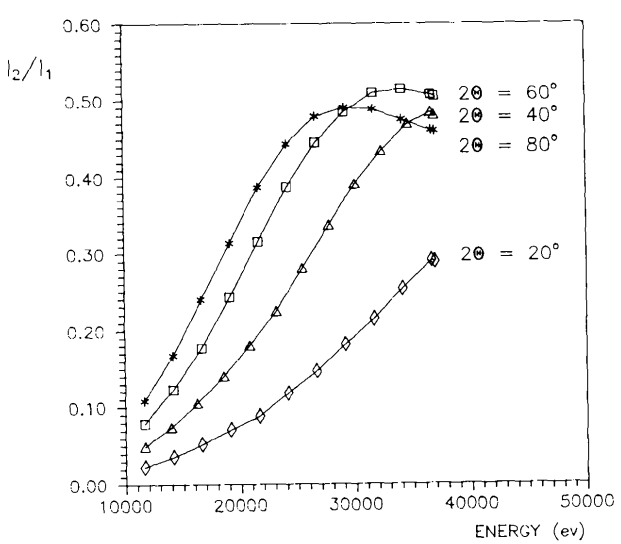

Fig. 3. Ratio of the intensities of double and single coherent scattering, I_2/I_1, for SiO_2 glass at different diffraction angles: $2\theta = 20°$ (◇); $2\theta = 40°$ (△); $2\theta = 60°$ (□); $2\theta = 80°$ (*).

is estimated by computing the integral

$$\int_0^{s_{max}} s^2[i(s) - 1]\, ds, \qquad (13)$$

where $s_{max} = (1.0135E_{max}) \sin \theta_{max}$, which should equal $-2\pi^2\rho_0$ according to the so-called sum rule (Wagner, 1978).

The reduced Faber–Ziman interference function, $s[i(s) - 1]$, for silica glass, obtained from the EDXD data shown in Fig. 4, is presented in Fig. 6 for the cases with and without the multiple scattering correction. Both interference functions agree well with each other in shape and numerical values, which indicates that the multiple-scattering correction appears to be insignificant in the radial-distribution-function analysis of SiO_2 glass by the EDXD method described here. The reason is that the multiple-scattering contribution to the EDXD data, when not explicitly accounted for, is absorbed by estimation of the incident-radiation-beam intensities $I_p(E)$ (see Fig. 2) and is thus compensated for to a great extent. We consider this self-correction to be an advantage of the computational procedures employed. It is worth mentioning that the interference function for silica glass shown in Fig. 6 agrees well with those for similar samples obtained by the ADXD method (Mozzi & Warren, 1969) and by the EDXD method (McKeown, 1987), which proves the reliability of the EDXD data processing performed here.

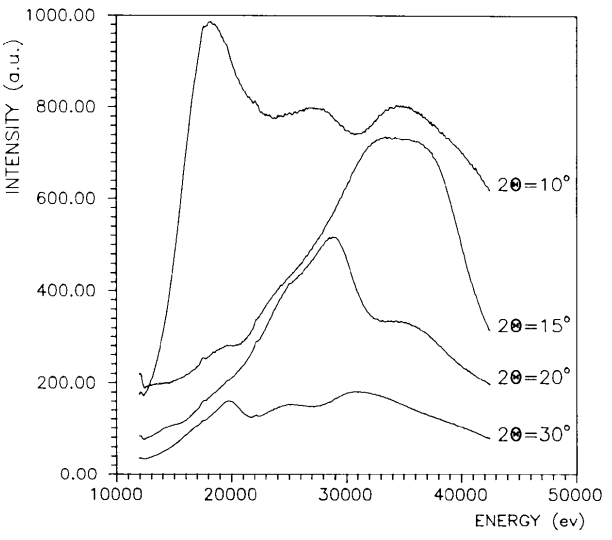

(a)

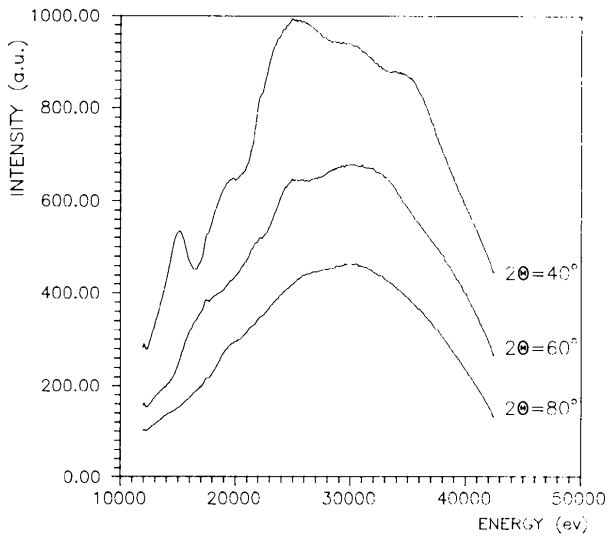

(b)

Fig. 4. EDXD profiles from silica glass obtained at: (*a*) low diffraction angles; (*b*) high diffraction angles.

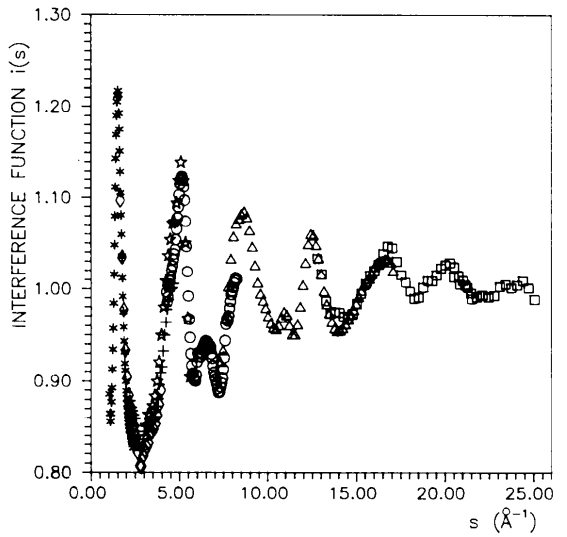

Fig. 5. Segments of the Faber Ziman type interference function of silica glass determined from EDXD data obtained at: $2\theta = 80$ (□); $2\theta = 60$ (△); $2\theta = 40$ (○); $2\theta = 30$ (☆); $2\theta = 20$ (+); $2\theta = 15$ (◇); $2\theta = 10$ (*).

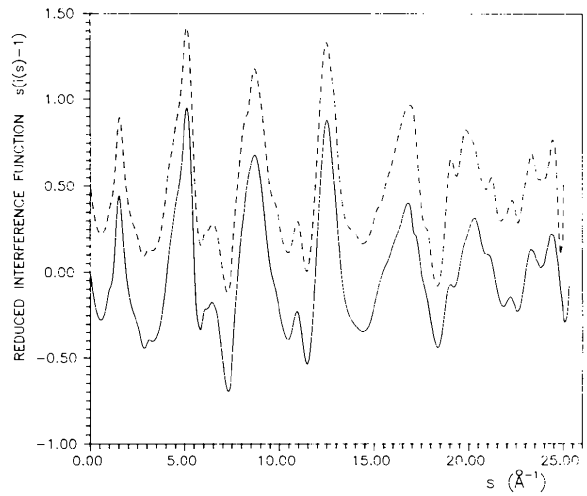

Fig. 6. Reduced interference functions for silica glass obtained from the EDXD data of Fig. 4, corrected (——) and not corrected (– – –) for multiple scattering.

3.5. *The DISTRF subroutine*

The reduced radial distribution function $G(r)$, the pair distribution function $g(r) = \rho(r)/\rho_0$ and the radial distribution function $4\pi r^2\rho(r)$ of the Faber–Ziman or Ashcroft–Langreth type as desired are computed by the Fourier transformation of the interference function [see (2)] in the *DISTRF* subroutine. The data for all the distribution functions are stored in a data file for further analyses. The quality of the distribution functions calculated is tested by fitting a straight line to $G(r)$ in the range $r = 0$–1 Å, to obtain the average atomic number density ρ_0, on the basis of

$$G_{FZ}(r) = -4\pi r\rho_0, \tag{14}$$

where $G_{FZ}(r)$ is a reduced radial distribution function of the Faber–Ziman type, and

$$G_{AL}(r) = -4\pi r\rho_0[\sum c_i f_i(s=0)]^2/\sum c_i f_i^2(s=0), \tag{15}$$

where $G_{AL}(r)$ is a reduced radial distribution function of the Ashcroft–Langreth type, which only holds for small values of r (Wagner, 1978). This is based on the physical reasoning that $\rho(r)$ should be zero in the region where the atoms do not approach each other, owing to the repulsion of the interatomic pair potential.

$G_{FZ}(r)$, for silica glass, evaluated from the interference function corrected for coherent multiple scattering, is shown in Fig. 7. That calculated from the interference function not corrected for multiple scattering is, in practice, indistinguishable from it and that is why it is not shown. The $G_{FZ}(r)$ obtained has a resolution superior to that of the $G(r)$ functions reported by Mozzi & Warren (1969) and McKeown (1987), since the interference function $i_{FZ}(s)$ has been determined up to the higher-s region and the use of any artificial damping factor is not required for the Fourier transformation.

Some factors that are unaccountable for, including the termination effect in the Fourier transformation, may cause spurious oscillations in $G(r)$, particularly in the region below the first peak, as one can see in Fig. 7. A procedure for modifying such residual problems, in a way similar to that proposed by Kaplow, Strong & Averbach (1965), is available in the program *PEDX*.

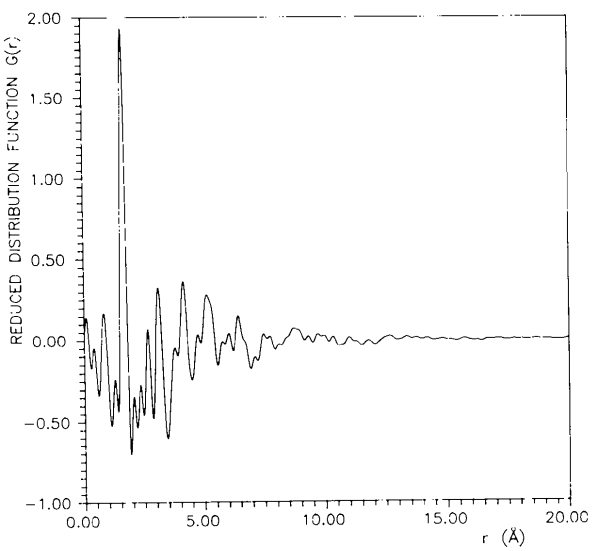

Fig. 7. Reduced radial distribution function for silica glass, calculated from the corrected interference function of Fig. 6.

PEDX has also been successfully tested using the EDXD data of $Fe_{40}Ni_{40}P_{14}B_6$ metallic glass and liquid mercury. A detailed description of the experimental set-up and procedures as well as a discussion of the results of radial-distribution-function analysis of the EDXD data obtained will be given elsewhere.

4. Implementation of *PEDX*

The program *PEDX* has been written in Microsoft Fortran77 and in its present version consists of 5000 statements. The program has been designed for IBM XT/AT or compatible personal computers equipped with a CGA/EGA/VGA graphics card. *PEDX* runs under PC/MS-DOS 4.0 (or later versions) and occupies about 400 kbytes of core memory. Despite the complexity of its computing scheme, the program is a high-performance one, so a sequence of data analysis takes only minutes to complete on an IBM AT with 80287 coprocessor. During the data processing, all important intermediate results and the final results are displayed on screen by means of a built-in graphics routine assembled from standard graphics functions included in the Microsoft Fortran Graphics Library. User interventions are scarcely needed in the course of the program execution. Data input and program-control operations are carried out through the keyboard in an interactive mode. With this architecture, the program is easy to use and requires no special knowledge of computers on the part of the user.

Copies of the *PEDX* program can by obtained from the authors.

The authors are indebted to Dr K. Sugiyama of Tohoku University, Sendai, and Dr S. Takeda, ERATO, JRDC, for valuable discussions and help in the EDXD experiments.

References

AUR, S. (1981). PhD thesis, Univ. of Pennsylvania, USA.
AUR, S. & EGAMI, T. (1980). *J. Phys. (Paris) Colloq.* **41**, C8, 234–237.
CROMER, D. (1969). *J. Chem. Phys.* **50**, 4857–4859.
CROMER, D. & MANN, J. (1967). *J. Chem. Phys.* **47**, 1892–1893.
CROMER, D. & WABER, J. (1965). *Acta Cryst.* **18**, 104–109.
EGAMI, T. (1978). *J. Mater. Sci.* **13**, 2587–2599.
EGAMI, T. (1979). *J. Appl. Phys.* **50**, 1564–1569.
FRITCH, G. & WAGNER, C. N. J. (1986). *Z. Naturforsch. Teil B*, **62**, 189–194.
FUKAMACHI, T., TOGAWA, S. & HOSOYA, S. (1973). *J. Appl. Cryst.* **6**, 297–298.
HANSON, C. D. & EGAMI, T. (1986) *J. Non-Cryst. Solids*, **87**, 171–184.
HOSOKAWA, S., MATSUOKA, T. & TAMURA, K. (1991). *J. Phys. C*, **3**, 4443–4457.
HOVING, W. (1986). PhD thesis, Univ. of Groningen, Germany.

HOVING, W., EGAMI, T., VINCZE, I. & WOUDE, F. (1987). *J. Phys. E*, **20**, 188–192.
KAPLOW, R., STRONG, S. & AVERBACH, B. (1965). *Phys. Rev. Sect. A*, **138**, 1336–1345.
MCKEOWN, D. A. (1987). *Phys. Chem. Glasses*, **28**, 156–163.
MALET, P. G., CABOS, C., ESCANDE, A. & DELORD, P. (1973). *J. Appl. Cryst.* **6**, 139–144.
MOMIUCHI, M. (1986). *J. Phys. Soc. Jpn*, **55**, 200–206.
MOZZI, R. & WARREN, B. (1969). *J. Appl. Cryst.* **2**, 164–172.
MURATA, Y. & NISHIKAWA, K. (1978). *Bull. Chem. Soc. Jpn*, **51**, 411–418.
NISHIKAWA, K. & IIJIMA, T. (1984). *Bull. Chem. Soc. Jpn*, **57**, 1750–1759.
OLSEN, J., BURAS, B., JENSEN, T., ALSTRUP, O., GERWARD, L. & SELSMARK, B. (1978). *Acta Cryst.* A**34**, 84–87.
OZAWA, H. & UNO, R. (1986). *J. Appl. Cryst.* **19**, 395–399.
PROBER, J. M. & SCHULTZ, J. M. (1975). *J. Appl. Cryst.* **8**, 405–414.
SAVITZKY, A. & GOLAY, M. J. E. (1964). *Anal. Chem.* **36**, 1627–1640.
TAMURA, K. (1990). *J. Non-Cryst. Solids*, **117/118**, 450–459.
THIJSSE, B. (1984). *J. Appl. Cryst.* **17**, 61–76.
UNO, R. & ISHIGAKI, J. (1984). *J. Appl. Cryst.* **17**, 154–158.
UTZ, R., BRUNSCH, A., LAMPARTER, P. & STEEB, S. (1989). *Z. Naturforsch. Teil A*, **44**, 1201–1209.
WAGNER, C. N. J. (1978). *J. Non-Cryst. Solids*, **31**, 1–40.
WAGNER, C. N. J., LEE, D., TAI, S. & KELLER, L. (1981). *Adv. X-ray Anal.* **24**, 245–252.
WASEDA, Y. (1980). *The Structure of Non-Crystalline Materials*, pp. 7–17, 27–36. New York: McGraw-Hill.
WASEDA, Y. (1984). In *Novel Applications of Anomalous X-ray Scattering for Structural Characterization of Disordered Materials. Lecture Notes in Physics*, Vol. 204. Berlin: Springer-Verlag.

J. Appl. Cryst. (1993). **26**, 302–304

An effective algorithm for calculation of the Clebsch–Gordan coefficients.

By LIANG ZUO,* MICHEL HUMBERT and CLAUDE ESLING, *Laboratoire de Métallurgie des Matériaux Polycrystallins, ISGMP, Université de Metz, F*-57045 *Metz CEDEX* 01, *France*

(*Received* 9 *June* 1992; *accepted* 4 *November* 1992)

Abstract

An algorithm to calculate the numerical values of the Clebsch–Gordan (C–G) coefficients is described. It uses a well elaborated recursive procedure yielding significantly high computation efficiency and accuracy. A 60-line Fortran program that implements the algorithm can be applied to the calculation of various symmetry-adapted C–G coefficients.

Introduction

In the quantum theory of angular momentum (Messiah, 1964), one often encounters the irreducible representation of the product of two generalized spherical harmonics:

$$T_{l_1}^{m_1 n_1}(g) T_{l_2}^{m_2 n_2}(g) = \sum_{l=|l_1-l_2|}^{l_1+l_2} (l_1 l_2 m_1 m_2 | l m)(l_1 l_2 n_1 n_2 | l n) T_l^{mn}(g)$$
$$(m = m_1 + m_2;\ n = n_1 + n_2), \quad (1)$$

where $(l_1 l_2 m_1 m_2 | l m)$ are the C–G coefficients defined by

$$\begin{aligned}(l_1 l_2 m_1 m_2 | l m) = \{&[(2l+1)/(l_1 + l_2 + l + 1)!] \\ &\times (l_2 + l - l_1)!(l + l_1 - l_2)!(l_1 + l_2 - l)! \\ &\times (l_1 + m_1)!(l_1 - m_1)!(l_2 + m_2)! \\ &\times (l_2 - m_2)!(l + m)!(l - m)!\}^{1/2} \\ &\times \sum_z [(-1)^z / z!][(l_1 + l_2 - l - z)! \\ &\times (l + z - l_1 - m_2)!(l_2 + m_2 - z)! \\ &\times (z + l - l_2 + m_1)!(l_1 - m_1 - z)!]^{-1}. \quad (2)\end{aligned}$$

In the sum, z traverses positive integers greater than or equal to $m_2 + l_1 - l$ and $l_2 - l - m_1$ and smaller than or equal to $l_1 + l_2 - l$, $l_2 + m_2$ and $l_1 - m_1$.

Many methods have been described of calculating the numerical values of the C–G coefficients, using either the general expression (2) (Simon, Vander Sluis & Biedenharn, 1954; Academia Sinica, 1965; Caswell & Maximon, 1969) or a recurrence scheme (Raynal, 1987). The aim of our work is to develop a new recursive procedure that minimizes required memory and computation time.

Mathematical aspects

The properties of the C–G coefficients have been extensively studied in the literature (Edmonds, 1960; Messiah, 1964). Only those related to our method are summarized here.

(1) *Selection rules*

For the nonzero C–G coefficients the following conditions must be fulfilled:

$$\begin{aligned} -l_1 \le m_1 \le l_1 \\ -l_2 \le m_2 \le l_2 \\ |l_1 - l_2| \le l \le l_1 + l_2 \\ -l \le m \le l \\ m = m_1 + m_2. \end{aligned} \quad (3)$$

* Permanent address: Department of Materials Science and Engineering, Northeast University of Technology, Shenyang 110006, People's Republic of China.

0021-8898/93/020302-03$06.00